Opposite effects of aerosols and meteorological parameters on warm clouds in two contrasting regions over eastern China

5 Yuqin Liu[1,4], Tao Lin[1,4], Jiahua Zhang[2], Fu Wang[3], Yiyi Huang[1], Xian Wu[1], Hong Ye[1], Guoqin Zhang[1], Xin Cao[1,4], Gerrit de Leeuw[5,6]

1 Key Lab of Urban Environment and Health, Institute of Urban Environment, Chinese Academy of Sciences, Xiamen 361021, China

2 Key Laboratory of Digital Earth Sciences, The Aerospace Information Research Institute, Chinese Academy of Sciences, Beijing 100094, China

3 CMA Earth System Modeling and Prediction Centre (CEMC), Beijing 100081, China

10 4 Fujian Key Laboratory of Digital Technology for Territorial Space Analysis and Simulation, Fuzhou 350108, China

5 Royal Netherlands Meteorological Institute (KNMI), R&D Satellite Observations, 3730AE De Bilt, The Netherlands

6 Aerospace Information Research Institute, Chinese Academy of Sciences (AirCAS), No.20 Datun Road, Chaoyang District, Beijing 100101, China

Correspondence to: Gerrit de Leeuw(gerrit.de.leeuw@knmi.nl), Tao Lin (tlin@iue.ac.cn)

15 **Abstract.** Aerosol and cloud properties retrieved from the Moderate Resolution Imaging Spectroradiometer (MODIS) on-board the Aqua satellite were used to investigate aerosol-cloud interaction (ACI) over eastern China, using aerosol optical depth (AOD) as a proxy for the aerosol concentration, during a period of 15 years (2008-2022). Two contrasting areas were selected: the heavily polluted Yangtze River Delta (YRD) and a clean area over the East China Sea (ECS). Linear regression

20 analysis shows the opposite behaviour of the cloud droplet effective radius (CER) and AOD relationship in the two different aerosol regimes. CER decreases with the increase of AOD in the moderately polluted atmosphere (0.1<AOD<0.3) over the ECS, in agreement with the Twomey effect. However, in the polluted atmosphere (AOD>0.3) over the YRD, CER increases with increasing AOD. Evaluation of the ACI index (here defined as the change in CER as a function of AOD) as function of the cloud liquid

25 water path (LWP) shows that in the moderately polluted atmosphere over the ECS the ACI index is significant and positive in the LWP interval [40 g m^{-2}, 200 g m^{-2}], and increases substantially with increasing LWP. In contrast, in the polluted atmosphere over the YRD the ACI index is significant and negative in the LWP interval [0 g m^{-2}, 120 g m^{-2}] and does not change notably as function of LWP in this interval. To further analyse the influence of AOD and meteorological conditions on cloud parameters,

30 the geographical detector method (GDM) has been used. The results show that all factors have a significant influence on the cloud parameters over the ECS, except for cloud top pressure (CTP), but the influence of AOD is larger than that of any of the meteorological factors. Among the meteorological

factors, lower tropospheric stability (LTS) has the largest influence on the cloud parameters and relative humidity (RH) the smallest. Over the YRD, the explanatory power of the effect of AOD and meteorological parameters on cloud parameters is much smaller than over the ECS, except for RH which has a statistically significant influence on CTP and can explain 65% of the variation of CTP. The combined effect of meteorological factors and AOD on cloud parameters enhances the explanatory power over the effect of individual parameters. The study further shows that over the ECS the effect of RH and LTS on the CER/AOD relationship is opposite to that of pressure vertical velocity (PVV). Over the YRD, The CER is larger in unstable atmospheric conditions than in stable conditions, irrespective of the AOD and the CER is much larger in high relative humidity conditions than in low relative humidity conditions.

Key words: AOD, Cloud parameters, LWP, Geographical detector method, MODIS, East China

1 Introduction

The atmosphere is primarily composed of gases, i.e. nitrogen, oxygen and several noble gases, as well as a wide variety of trace gases that occur in relatively small and highly variable amounts. In addition, liquid and solid particles are suspended in the atmosphere. The suspension of solid and liquid particles in the gaseous medium is technically defined as an aerosol, but in practice the term aerosol refers to the particulate component only (Seinfeld and Pandis, 1998). The aerosol particles originate from a large variation of both direct and indirect sources and their chemical and physical properties change under the influence of atmospheric processes, which thus are variable in space and time. Directly emitted aerosol types include, e.g., sea spray, dust, smoke, volcanic ash, pollen etc. The indirect formation of aerosol particles occurs through nucleation and subsequent growth by physical and chemical processes such as condensation, coagulation and multiphase chemical reactions on the particle surface, involving precursor gases such as SO_2, NO_2, NH_3, volatile organic compounds (VOCs), etc. Aerosol particles are important for climate, air quality and heterogenous chemical processes. Aerosol particles exert a direct effect on climate by scattering incoming solar radiation back into space, which results in cooling and reduction of the warming effect of greenhouse gases (GHG), while the interaction of absorbing aerosol particles with solar radiation may result in local heating and thus reinforce the GHG effect and influence meteorological processes. Aerosol particles can act as cloud condensation nuclei or ice nuclei, depending on their chemical composition and size; when they are activated they can exert an indirect effect on climate by

changing the cloud microphysical properties and precipitation (Tao et al., 2012; Fan et al., 2016; Rosenfeld et al., 2019; Rao and Dey, 2020; Bellouin et al., 2020). The first indirect effect of aerosols, often referred to as the "Twomey" effect (Twomey, 1977; Matheson et al., 2005; Koren et al., 2005; Meskhidze and Nenes, 2010; Costantino et al., 2010; 2013), describes the effect of the increase of the

65 number of aerosol particles when the cloud liquid water path (LWP) remains unchanged, which results in the increase in the number of cloud droplets and the decrease of the cloud droplet effective radius (CER). The smaller CER in turn results in the enhanced reflection of solar radiation (Twomey, 1977; Feingold, et al., 2001). The second indirect effect describes the decrease in precipitation efficiency due to the decrease in the size of the cloud droplets, resulting in the increase of the LWP and the amount of

70 clouds, thus enhancing the reflection of solar radiation (Albrecht, 1989). The first and second indirect effects are also referred to as the cloud albedo and cloud lifetime effects (Quaas et al., 2008). The CER is an important factor affecting cloud physical processes and optical properties, which in turn influence precipitation and the Earth' radiation balance. Slingo (1990) pointed out that a reduction in the average CER by 15% - 20% can balance the radiative forcing at the top of the atmosphere caused by a doubling

75 of carbon dioxide. Therefore, small changes in cloud microphysical properties may lead to important climate impacts (Zhao et al., 2018). Further study on the relations between aerosols and CER, together with meteorological parameters influencing aerosol-cloud interaction, can improve our understanding of these processes leading to improved aerosol-cloud parameterizations in regional climate models.

The effects of aerosols on the microphysical characteristics of clouds have been studied based on data

80 from a large number of monitoring campaigns, using satellite, aircraft and ground based observations, and by using model simulations. Because of the large spatial coverage and high spatial and temporal resolution, satellite instruments have been widely used to study aerosol-cloud interaction in different conditions, confirming the large influence of aerosol particles on cloud properties (e.g., Yuan et al., 2008; Rosenfeld et al., 2014; Saponaro et al., 2017; Liu et al., 2018; Pandey et al., 2020; Christensen et al.,

85 2020; Liu et al., 2021). In studies of the first indirect effect of aerosols with satellite data, the aerosol optical depth (AOD) is used as a proxy for the aerosol concentration. Many of these studies confirm the Twomey effect (Chen et al., 2014; Christensen et al., 2016; Jia et al., 2019). However, other studies show that, over some areas and especially over land in situations with high AOD, the CER increases with the increase of AOD, in contrast to the hypothesis of the "Twomey effect" (Feingold et al., 2001; Grandey

90   and Stier, 2010; Wang et al., 2015; Jia et al., 2019; Liu et al., 2020). It is noted that in these studies, the

relationship between CER and aerosol concentration was not constrained by LWP, although this is the

premise of the first indirect effect of aerosol.

Meteorological conditions are important factors determining both the occurrence of clouds and cloud

properties and therefore, in aerosol-cloud interaction (ACI) studies, the variation of meteorological

95   conditions needs to be considered together with the variation of AOD. Su et al. (2010) studied the

influence of pressure vertical velocity (ω_{700hPa}) on the first indirect effect of aerosols and demonstrated

the effect of this parameter on the CER and the LWP. Gryspeerdt et al. (2014) studied the relationship

between aerosol and initial cloud cover as a function of relative humidity (RH_{850hPa}) and vertical

convection strength (ω_{500hPa}). Wang et al. (2014) proved that the well-recognized aerosol effect mingled

100   with meteorological conditions (RH_{750hPa} and ω_{750hPa}), which likely is the main reason for the positive

aerosol cloud interaction (ACI) index (defined in Section 3.1) over land. Wang et al. (2015) discussed

the increase of CER with AOD in high AOD conditions over eastern China, which was observed during

the summer but not in the winter, in terms of meteorological conditions. In particular they considered the

different humidity effects during these seasons. Liu et al. (2017) showed that the formation of large cloud

105   droplets in both horizontal and vertical directions and the increase in cloud cover are promoted in an

environment with high relative humidity (RH_{950hPa}). A rising air mass (ω_{750hPa}) can promote the formation

of thicker and higher clouds.

Only few studies have addressed the influence of different aerosol and meteorological parameters on the

aerosol indirect effect and most of them used traditional statistical methods. In the current study the

110   geographical detector method (GDM) is applied to quantify the relative importance of the effects of nine

parameters on ACI. The GDM is a set of statistical methods to detect the spatial variability of aerosol

and cloud properties, which are spatially differentiated, and evaluate the occurrence of correlations in

their behaviour and the driving forces behind these correlations (Wang and Hu, 2012; Wang et al., 2016).

The basic idea of the GDM is that the spatial distributions of two variables tend to be similar if these two

115   variables are connected (Zhang and Zhao 2018). The method can be used to analyse the relative

importance of influencing factors on ACI.

The focus of the current study is to establish a CER-aerosol parameterization scheme by the application

of the GDM to satellite data over two contrasting areas, i.e. the Yangtze River Delta (YRD) in eastern

China, with high aerosol concentrations, and a relatively clean area over the East China Sea (ECS). The satellite data are first used to build a relationship between CER and the aerosol concentration (using AOD as a proxy) for different AOD regimes and all LWP values, followed by constraining the LWP in different intervals. Next the GDM is applied to determine the relative effects of different parameters on the ACI. Relations between CER and AOD, meteorological conditions and several cloud properties are analysed, including combined effects of different influencing parameters.

2 Approach

2.1 Study area

The complex aerosol composition and the high aerosol concentrations render eastern China an interesting area for a variety of studies of processes involving aerosols, including the current study on the use of satellite data for the systematic assessment of aerosol indirect effects. The ACI study focuses on two areas, i.e. the Yangtze River Delta (YRD, 27°N-35°N; 114°E-122°E) in eastern China and the East China Sea (ECS, 20°N-28°N; 126°E-134°E). The locations of the YRD and the ECS are shown in the map in Figure 1.

The YRD has a developed economy, with much industrial activity, large harbors (sea and river) and related busy ship traffic, dense populations in large urban centers, all with high traffic intensity and high energy consumption. In addition to the direct emission of black carbon, also aerosol precursor gases such as NO_2, SO_2 and VOCs are emitted from the combustion of biomass, coal and petrochemical fuels, leading to the formation of secondary aerosol particles such as nitrate and sulfate aerosols, while agricultural activities result in the emission of dust, ammonia and biological VOCs (BVOCs) into the atmosphere. These activities and associated emissions result in the occurrence of high AOD over the YRD. Over the East China Sea (ECS) the main aerosol types are sea spray aerosol generated by the interaction between wind and waves and anthropogenic pollutants transported from the land in the East Asian outflow. During transport over hundreds of km, aerosol particles are removed by several processes such as dry and wet deposition and hence the aerosol concentrations decrease and the AOD becomes relatively low and is dominated by sea spray aerosol. In view of the differences in aerosol composition and concentrations, the polluted YRD area and the relatively clean ECS area were selected as contrasting regions for the study of the influence of aerosols on cloud properties over land and over ocean
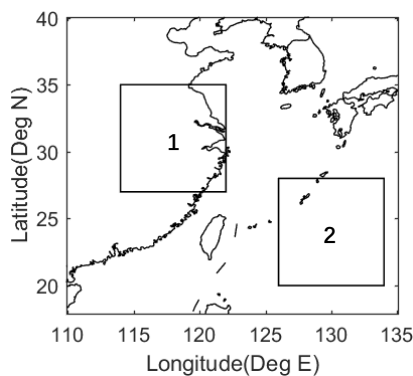
Figure 1. Map showing the locations of the two study areas selected for aerosol - cloud interaction studies: area 1 is the Yangtze River Delta (YRD; 27°N-35°N, 114°E-122°E), and area 2 indicates the selected Eastern China Sea (ECS) area (20°N-28°N, 126°E-134°E).

150

2.2 Data used

In this study, aerosol and cloud properties were used which were derived from measurements from the

Moderate Resolution Imaging Spectroradiometer (MODIS) on-board the Aqua satellite, for the period

2008-2022 (15 years). This data was selected because the MODIS data are widely used and therefore

155   they are well-characterized. In addition, the Aqua satellite flies in an afternoon orbit with local overpass

time around 13:30, when the atmospheric boundary layer is well-developed. MODIS L3 collection 6.1

daily   aerosol   and   cloud   parameters   were   downloaded   from   the   LAADS   website

(https://ladsweb.modaps.eosdis.nasa.gov/, last access: 12 July 2022) with a spatial resolution of 1°x1°.

The utilization of the daily MODIS aerosol and cloud data at 1°x1° resolution ensures that they are

160   coincident when investigating aerosol - cloud interaction. The MODIS instrument has 36 spectral bands

- aerosol properties are retrieved using the first seven of these (0.47-2.13 μm) (Remer et al., 2005; Levy

et al., 2013; Sayer et al., 2014) while additional wavelengths in other parts of the spectrum are used for

the retrieval of cloud properties (Platnick et al., 2003). More detailed information on algorithms for the

retrieval of aerosol and cloud properties is provided at http://modis-atmos.gsfc.nasa.gov (last access: 01

165   July 2021). In this study we use the AOD at 550 nm (referred to as AOD throughout this manuscript),

CER, cloud optical thickness (COT), cloud liquid water path (LWP), cloud top pressure (CTP), cloud

fraction (CF) and cloud top temperature (CTT). AOD is used as a proxy for the amount of aerosol

particles in the atmospheric column to investigate ACI (Andreae, 2009; Kourtidis et al., 2015). To reduce

a possible overestimation of the AOD (e.g., due to cloud contamination), cases with AOD greater than 1.5 were excluded from further analysis. As most aerosol particles are located in the lower troposphere (Michibata et al., 2014), the focus in this study is on warm clouds with CTT larger than 273K, CTP larger than 700 hPa and LWP smaller than 200 g m^{-2}. Transparent-cloudy pixels (COT<5) were discarded to limit uncertainties (Grosvenor et al., 2018). The solar zenith angle was restricted to SZA < 65° and the viewing zenith angle to VZA <55° to avoid the large biases in COT and CER retrievals at larger angles (Grosvenor et al., 2018). Cloud parameters were only considered in single liquid layer clouds.

Effects of meteorological conditions on ACI were explored using the daily temperature at the 700 and 1000 hPa levels, relative humidity (RH) at the 750 hPa level and pressure vertical velocity (PVV) at the 750 hPa level. Low tropospheric stability (LTS), which is defined as the difference in potential temperature between the free troposphere (700 hPa) and the surface (1000 hPa), is used as a measure of the strength of the inversion that caps the planetary boundary layer (Klein and Hartmann, 1993; Wood and Bretherton, 2006). These meteorological data were retrieved from the ECMWF ERA-5 reanalysis data which provide global meteorological conditions at 0.25°x0.25° resolution for 37 pressure levels in the vertical (1000-1 hPa), for every 1 h (UTC) (https://cds.climate.copernicus.eu/cdsapp#!/dataset/reanalysis-era5-pressure-levels-monthly-means?tab=form, last access: 12 July 2022). The meteorological parameters were resampled to the MODIS/Aqua overpass time at 13:30 (local time) by taking a weighted average of the properties at the two closest times (05:00 UTC and 06:00 UTC) provided by ERA Interim.

3 Methods

3.1 Aerosol-cloud interaction index

The first indirect effect of aerosols is defined as the variation of cloud optical or microphysical parameters (cloud optical thickness, cloud droplet effective radius, etc.) with the variation of aerosol loading. Aerosol particles can become cloud condensation nuclei (CCN) or ice nuclei (IN), depending on their chemical composition. When these nuclei are activated, they become cloud droplets due to condensation of water vapor. When the concentration of aerosol particles increases, often also the number of CCN or IN increases and thus the number of cloud droplets. However, if the liquid water content in the cloud does not change (as indicated by a constant LWP), the condensable water will be distributed over more cloud

droplets which thus remain smaller, i.e. the CER decreases and the cloud albedo increases when the

aerosol concentration increases. On the basis of findings of Kaufman and Fraser (1997), Feingold et al.

(2001) pointed out that the aerosol cloud interaction caused by the first indirect effect can be calculated

200   by the following formula:

$$IE=ACI_r=-\frac{d\ ln\ r_e}{d\ ln\ \alpha}|_{LWP} \quad 0 < ACI_r < 0.33 \quad (1)$$

Where r_e represents the cloud droplet effective radius (CER) and α represents the aerosol number

concentration. Equation (1) describes the change of CER with the change of the aerosol concentration

for constant LWP. In this study, the AOD is used as a proxy for the aerosol number concentration and

205   ACI_r can be determined as the slope of a linear fit to a log-log plot of CER versus AOD. It is noted that

ACI_r is a function of CER and effects on CER directly influence ACI_r. In this study effects on ACI_r (from

here on simply denoted as ACI) and CER are used intermittently.

3.2 Geographical detector method

The geographical detector method (GDM) is introduced to analyze which factors influence the ACI. The

210   GDM is based on the assumption that if an independent variable has an important influence on its

dependent counterpart, their spatial distributions should also have evident similarities (Wang and Hu,

2012; Wang et al., 2016). The geographical detector provides four modules, including the factor detector,

interaction detector, risk detector and ecological detector. In this study, the first two modules are used to

detect interactions between different parameters, based on their spatial variations, and thus reveal the

215   driving factors for aerosol-cloud interaction over the target regions. The influencing factors (x)

considered in this study are aerosol and meteorological parameters and the dependent factors (y) are the

ACI index and cloud parameters. In the GDM, for example, the CER data are recorded in a raster grid as

illustrated in Figure 2. The data in the raster grid is transformed into dot files, each dot containing a value

for the CER and for one of the influencing parameters x. The dependent (CER) and influencing (x)

220   parameters are separated into 2 layers with the same grid. In the x layer, the Jenks natural breaks

classification method (Brewer and Pickle, 2002), aiming to minimize the variance within the group and

maximize the variance between groups, was applied to categorize the whole region into N_i sub-regions

(3 in Figure 2), according to pre-defined ranges of influencing factors (e.g. AOD). In each spatial unit

(N_i), the influencing factor (x) varies within certain limits, with variance σ_i. The power of determination

225   q of x to y (also referred to as power of the influencing factor) determines the extent to which a factor x

influences the dependent factor (y) over the whole study area and is calculated using Equation (2):

$$q = 1 - \frac{\sum_i^L N_i \sigma_i^2}{N \sigma^2} \qquad (2)$$

where i (1, …, L) is the number of subregions of factor x; N represents the total number of spatial units

over the entire study area; N_i denotes the number of samples in subregion i; and σ_i^2 and σ^2 denotes

230   variance of samples in the subregion i and the total variance in the entire study area, respectively. The

value of q varies between 0 and 1, i.e. $q[0,1]$, where 0 indicates that factor x has no influence on y and

the closer q is to 1, the greater the influence of x. For instance, if $q = 0.5$, x can explain 50% of the

variation of y. In this study multi-years mean values of influencing factors (x) and dependent factors (y)

are calculated for each raster grid. Then, we classified the influencing factors (e.g. AOD and

235   meteorological parameters) into 5 subregions by the Jenks natural breaks classification method (Brewer

and Pickle, 2002).
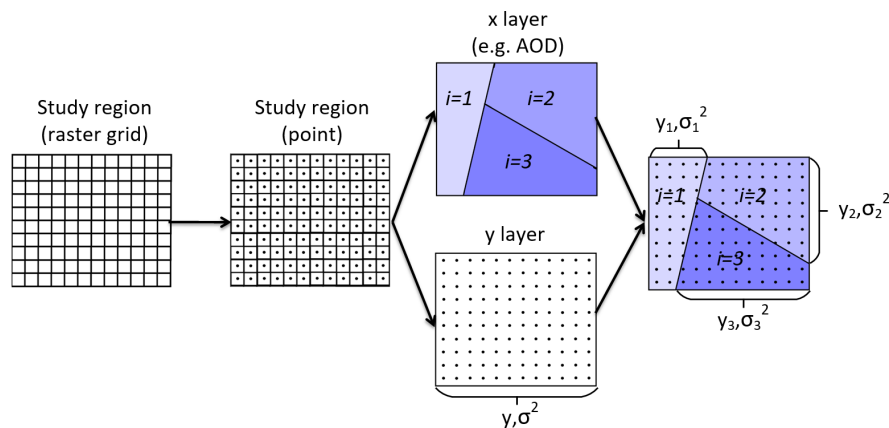
Figure 2. The principle of the geographical detector method. See text for explanation.

Usually, the dependent variable y is influenced by several different factors x_i (Figure 3) and the combined

240   effect of two or more factors may have a weaker or stronger influence on y than each of the individual

factors. The q values for the influences of factors x1 and x2 on y, obtained from the application of the

factor detector method (equation 2), may be represented as q (x1) and q (x2). Hence, a new spatial unit

and subregions may be generated by overlaying the factor strata x1 and x2, written as x1∩x2, where ∩

denotes the interaction between factor strata x1 and x2 as illustrated in Figure 3. Thus, the q value of the

245   interaction of x1∩x2 may be obtained, represented as q (x1∩x2). Comparing the q value of the interaction

of the pair of factors and the q value of each of the two factors, five categories of the interaction factor

relationship are described as summarized in Table 1.
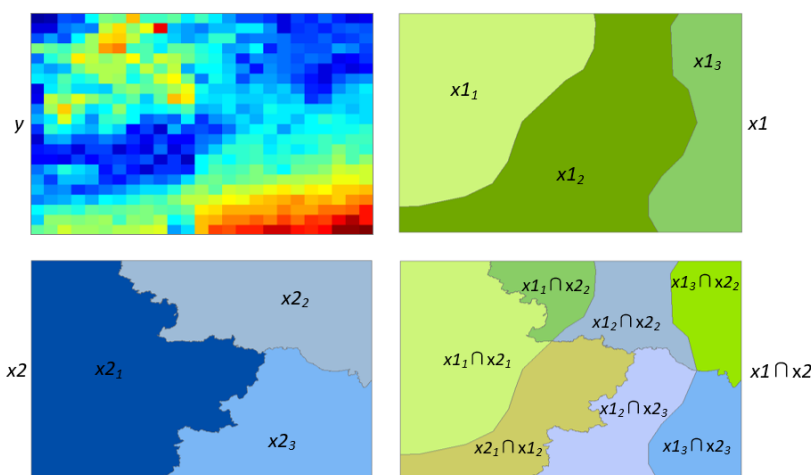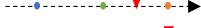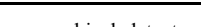
Figure 3. Detection of interaction.

250   **Table 1. Interaction categories of two factors and the interaction relationship**

	Description	Interaction
	$q(x1 \cap x2) < Min[q(x1),q(x2)]$	Weakened, nonlinear
	$Min[q(x1),q(x2)] < q(x1 \cap x2) < Max[q(x1),q(x2)]$	Weakened, unique
	$q(x1 \cap x2) > Max[q(x1),q(x2)]$	Enhanced, bilinear
	$q(x1 \cap x2) = q(x1)+q(x2)$	Independent
	$q(x1 \cap x2) > q(x1)+q(x2)$	Enhanced, nonlinear

The geographical detector method has been used to detect influencing factors for several different

purposes (Wang et al., 2018; Zhang and Zhao, 2018; Zhou et al., 2018). In the current study, this method

was used to detect the impact of nine variables and their interactions on the variations of ACI and cloud

parameters over land and ocean. The advantages of using the GDM in this approach are (1) stratified

255   independent variables enhance the representation of a sample unit, so it has higher statistical accuracy

than other models with the same sample size; (2) the use of a q-statistic value can afford a higher level

of explanatory power, but does not require the existence of a linear relationship between independent and

dependent variables; (3) the geographical detector can determine the true interaction between two

variables and is not limited to pre-established multiplicative interactions (Wang et al., 2010); (4) the use

260   of a geographical detector does not need to consider the collinearity of multiple independent variables

(Wang et al., 2010).

4 Results and Discussion

4.1 Spatial distribution and correlation analysis of AOD and cloud parameters

The spatial variations of the AOD and the cloud properties CER, COT, CF, CTP and LWP over the study area, averaged over the years 2008-2022, are presented in Fig. 4. Figure 4a shows a large difference between the AOD over land and ocean, with the highest values over the northern part of the YRD (averaged AOD larger than 0.5), and the lowest values over the southwestern part of the ECS (<0.1); the AOD decreases gradually from land to ocean. The spatial distributions of the CER, COT, CF, CTP and LWP) over the YRD and ECS in Figs. 4b–f shows that for each of them there is a distinct difference between those over land and over ocean both as regards the values and the spatial variation. Over the ECS, the CER is largest in the south and decreases toward the north of this area and the values are overall substantially larger than over the YRD, where the CER varies somewhat and decreases from north to south. The variation of the CER with AOD over the YRD is opposite to what would be expected, which will be discussed in Sect. 4.2. The COT also varies somewhat over the YRD but, contrary to the CER, COT increases from north to south. Over the ECS, the COT is generally lower than over the YRD, with the highest values in the NW which gradually decrease toward the SW. Clearly, the CER is higher and the COT is lower over the ECS than over the YRD.

The spatial distributions of CF, CTP and LWP are clearly different. Over the ECS, CF increases from the SW to the NW, opposite to the variations of the CTP and the LWP which are lower in the north of the ECS than in the south. Over ocean the clouds are generally lower (higher CTP) than over land, and CTP varies over the study area with the highest values over land, in the north. Over the YRD, the spatial patterns of the CF and CTP are opposite, with CF increasing from south to north and CTP decreasing. Over the YRD, the spatial distributions of COT and LWP are similar with higher values toward the south. Over the ECS, the LWP varies with the lowest values in the NW and the highest values in the south. The high values of the CER and CF over the ECS could be due to the dominance of sea spray aerosol, the high hygroscopicity of which makes these particles very efficient CCN.
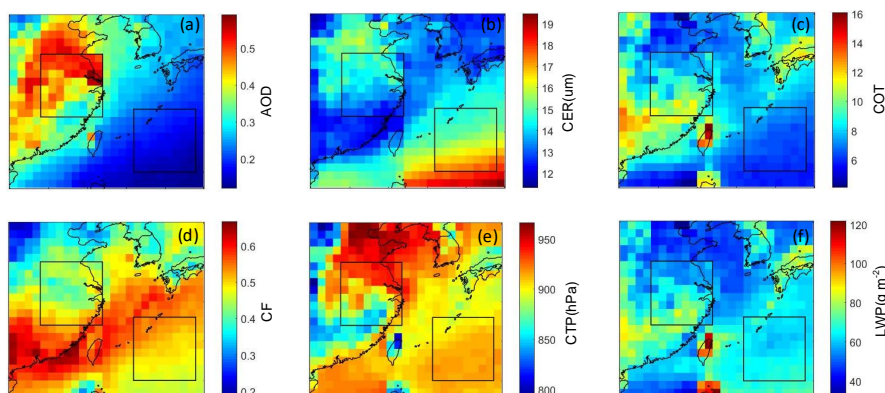
Figure 4. Spatial distributions of AOD (a), CER (b), COT (c), CF (d), CTP (e) and LWP (f), averaged over the years 2008 - 2022 over the study area, with the YRD and ECS marked by the squares.

4.2 ACI estimates for CER for the whole LWP regime

Equation (1) shows that the value of the ACI is determined by the slope of a linear fit to a log-log plot of CER versus AOD. To investigate the ACI, the data was binned in AOD intervals with a bin width of 0.02, and the CER data in each AOD bin were averaged. Logarithmic plots of the averaged CER data versus AOD over the YRD and the ECS are presented in Figure 5. Figures 5a (YRD) and 5b (ECS) show different regimes for the variation of the CER with the AOD. The first regime, for AOD ≤ 0.05, shows the increase of CER with AOD over both regions, followed by a variable CER over the YRD and a gradually stronger decrease over the ECS for AOD between 0.05 and 0.1. In view of this variability and the uncertainty of AOD of ± (0.05 + 15 %) over land and ± (0.03 + 5 %) over ocean (Levy et al., 2013), the ACI will not be investigated for AOD < 0.1. For higher AOD, the CER / AOD relation changes for AOD around 0.3. Thus, the second regime is selected as the part of the CER vs AOD for AOD between 0.1 and 0.3. In this AOD regime, the CER fluctuates a little with AOD over the YRD (Figure 5a) but the CER values remain within the standard deviation and the expected Twomey effect is not observed. In contrast, over the ECS the CER clearly decreases with AOD increasing from 0.1 to 0.3 (Figure 5b), in good agreement with expectation based on the Twomey effect, and the correlation between CER and AOD is high with R=0.99 and statistically significant. Note however, that no selection was made for LWP and the condition of constant LWP was not fulfilled. This will be further discussed in Section 4.3. In the third regime, where AOD > 0.3, CER increases with increasing AOD over the YRD, with correlation coefficient R= 0.9. In contrast, over the ECS the CER does not significantly change with

increasing AOD for AOD>0.3. However, the large uncertainty in the bin-averaged CER in this AOD

310   regime, increasing with increasing AOD, indicates a very variable ACI between high-AOD events which

on a statistical basis cannot be further analysed and likely depends on the type of aerosol present during

each event and the meteorological conditions. The reason for the positive relationship between CER and

AOD over the YRD may be similar to that described by Feingold et al. (2001), i.e., in the presence of a

large number of aerosol particles competing for a limited amount of water vapor, only a subset of aerosol

315   particles is activated. Once activated, these particles continue to grow faster, thus preventing water vapor

from condensing onto smaller aerosol particles that are less susceptible to activation. As a result, the

amount of available water vapor is distributed over a subset of aerosol particles which thus become cloud

droplets with relatively large CER and the CER in turn increases with further increasing AOD (Liu et al.,

2017).

320   The response of CER to AOD is stronger over the ECS (0.1<AOD<0.3) than over the YRD (AOD>0.3).

It is anticipated that during the relatively low AOD over the ECS during AOD regime 2 (AOD 0.1-0.3)

the aerosol number concentration is dominated by sea spray aerosol particles (de Leeuw et al., 2011)

which are hygroscopic and thus provide good CCN, while over open ocean also the relative humidity is

generally high. Hence the available water vapor will be readily distributed over all CCN, resulting in the

325   decrease of the CER and a strong correlation with AOD. Further, the AOD over open ocean does not

reach high values in the absence of continental influence, even in very high wind speeds the AOD does

not exceed 0.2 (Huang et al., 2010; Smirnov et al., 2012). Hence AOD higher than 0.2 over the ECS is

influenced by long-range transport of aerosol produced over land with lower hygroscopicity, and thus

lower susceptibility to act as CCN, which explains the breakdown of the Twomey effect over the ECS

330   for elevated AOD. In fact, the data in Figure 5b show that the CER/AOD relationship starts to flatten for

AOD ~0.2 and is flat for AOD larger than ~0.3. Overall, Figure 5 shows that the Twomey effect is clear

in the second AOD regime over the ECS and in the third AOD regime over the YRD. For this reason,

the further analysis focuses on the ACI over the ECS for AOD between 0.1 to 0.3, and over the YRD for
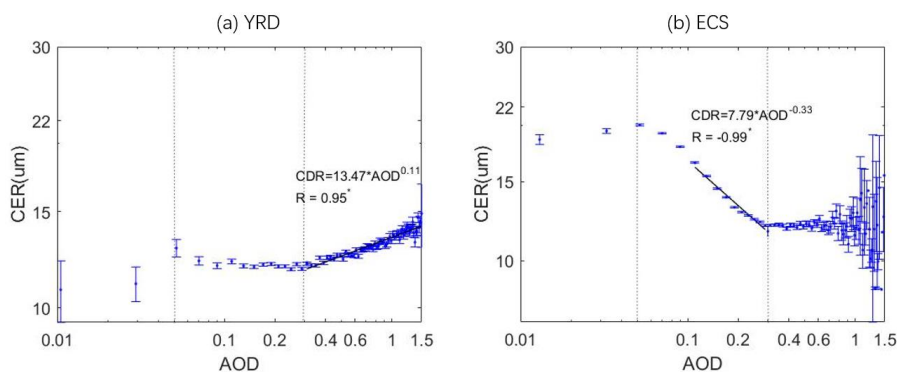
AOD > 0.3.

335

Figure 5. Variation of CER with AOD over the YRD (a) and ECS (b). Here all CER data were averaged in AOD bins, from 0.0 to 1.5 with a step of 0.02. Note that the data are plotted on a log-log scale. The lines for the YRD data for AOD>0.3 and for the ECS data for 0.1<AOD<0.3 represent least-square fits to the binned data, and the resulting relations are presented in each figure. The marker ∗ at the top right corner of the R

340   **value indicates that the correlation is statistically significant with p < 0.05. The thin vertical lines indicate the AOD regimes as explained in the text.**

To study the spatial variation of the ACI over the study area, the ACI in each grid cell has been calculated by application of Equation (1) to all observations over the YRD for which AOD>0.3 and to all observations over the ECS for which 0.1<AOD<0.3. The results are plotted in Figure 6, which shows

345   maps of the ACI, the correlation coefficient R and the statistical P-value for each grid cell over the study area. Figure 6b shows that the ACI over the ECS, for the second AOD regime (0.1-0.3) is positive, with large negative correlation coefficients (-0.78~-0.99) which mostly are statistically significant. These results show the good correlation between CER and AOD, consistent with the theory of the first AIE. In contrast, over the YRD, for the third AOD regime (>0.3), the ACI is mostly negative and the correlation between CER and AOD is positive, i.e. high aerosol loading results in larger CER for AOD>0.3, as was

350   also concluded from Figures 5a and b. The data in Figure 6a show that the negative CER/AOD relation is strongest in the part of the selected YRD region north of Shanghai but R is relatively small (0~0.63) and for the majority of the cells the statistical significance is ~0.1 or larger. In the part of the selected YRD region south of Shanghai the correlations are small and not statistically significant. The observed

355   anti-Twomey effect of aerosols over the YRD has also been reported in earlier publications such as Jin and Shepherd (2008), Yuan et al. (2008) and Liu et al. (2017). Factors influencing the relationship between AOD and cloud parameters have been reported in the literature, such as hygroscopic effects (e.g., Qiu et al., 2017), atmospheric stability, cloud dynamics, cloud height (Shao and Liu, 2005) and land

cover type (Jin and Shepherd, 2008; Ten Hoeve et al., 2011). The effects of competing mechanisms and

360   their possible influence on the observed response of CER to high AOD in the YRD will be further

discussed in the following sections.
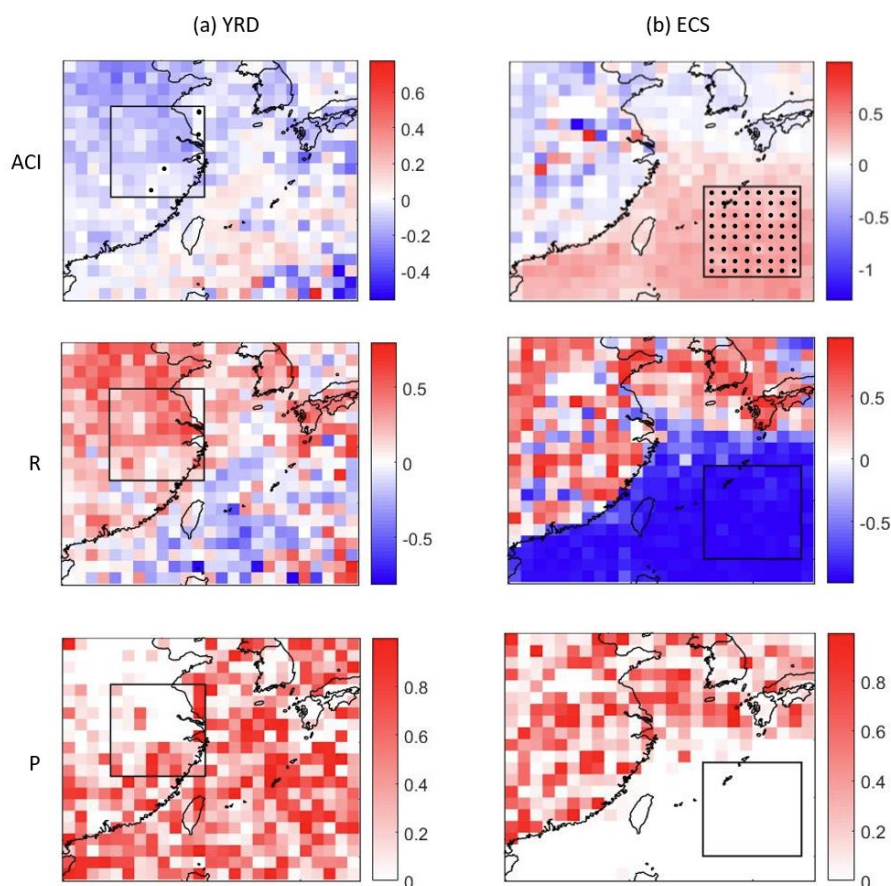
**Figure 6. Using the AOD as a proxy for aerosol concentrations, estimates of the ACI for CER were calculated
for each grid point. Maps of the spatial distributions of the ACI, the correlation coefficients and the statistical**

365   **P-values in each grid point are presented in Figure (a) for the YRD for the AOD regime with AOD>0.3 and in
Figure (b) over the ECS for the AOD regime with 0.1<AOD<0.3. ACI, R and P-values are color coded
following the color bars at the right of each figure. The black solid dots indicate that the ACI value is positive
in the grid point over the YRD and ECS.**

4.3 ACI estimates for CER for different LWP regimes

370   In the data presentation and discussion in Section 4.2, the condition of constant LWP (Equation 1) was

not considered. Because constant LWP is a condition for the application of eq. (1) to calculate ACI, in

this Section the effect of LWP will be further investigated. To this end, the condition of constant LWP is approached by considering five LWP intervals, each with a width of 40 g m^{-2}, the range of [0 g m^{-2}, 200 g m^{-2}]. The ACI in the whole area was calculated for each LWP interval using Equation (1) for all

375   observations over the YRD for which AOD>0.3 and all observations over the ECS for which 0.1<AOD<0.3. The results are presented in Table 2, together with the corresponding correlation coefficients R for the relation between the CER and AOD in the relevant AOD regimes. The significance of these correlations was determined by using the student's t test, i.e. the results are statistically significant when the p value is smaller than 0.01, where p is defined as the probability of obtaining a

380   result equal to or "more extreme" than what was actually observed. The data in Table 2 show that over the ECS the ACI estimates are positive and statistically significant for all four LWP ranges between 40 and 200 g.m^{-2}, and increase with increasing LWP from 0.17 (LWP 40-80 g.m^{-2}) to 0.42 in the highest LWP range (160-200 g.m^{-3}), with corresponding R of -0.98 to -0.99. Thus the magnitude of the LWP has a substantial influence on the aerosol effect on the ACI. Over the YRD, the ACI is significant in the first

385   three LWP regimes, with the ACI varying between -0.10 and -0.13, with a correlation R between 0.76 and 0.96. These data show that over the YRD the LWP effect on the ACI is smaller than over the ECS and, in contrast to the ECS, over the YRD the magnitude of the LWP has little influence on the strength of the ACI.

In summary, the data show that both over the ECS and the YRD the relationships between the CER and

390   the AOD are significant, but for different LWP intervals ([0 g m^{-2}, 120 g m^{-2}] over the YRD and [40 g m^{-2}, 200 g m^{-2}] over the ECS) and for different AOD regimes (0.1<AOD<0.3 over the ECS and AOD>0.3 over the YRD), and that the ACI follows the Twomey effect over the ECS and the anti-Twomey effect over the YRD.

In the following study on the effects of the AOD and different cloud and meteorological properties on

395   the ACI, using the GDM, these differences will be taken into account, i.e. over the YRD only data with AOD > 0.3 and LWP in the range from 0 to 120 g m^{-2} will be used and over the ECS only data with AOD in the interval [0.1, 0.3] and LWP in the range from 40 to 200 g m^{-2} will be used.

400

Table 2. ACI estimates and correlation coefficients R or the CER-AOD relationships in five different LWP intervals computed using Equation (1) over ECS for 0.1<AOD<0.3 and over the YRD for AOD>0.3. Statistically significant data points are indicated with * (p value < 0.01)

	ECS (0.1<AOD<0.3)		YRD (AOD>0.3)	
LWP	ACI	R	ACI	R
0-40	-0.13	0.99*	-0.12	0.91*
40-80	0.17	-0.98*	-0.13	0.96*
80-120	0.35	-0.99*	-0.10	0.76*
120-160	0.41	-0.99*	0.01	-0.10
160-200	0.42	-0.99*	0.08	-0.37*

4.4 Geographical detector model analysis

4.4.1 Factor detector analysis

The GDM factor detector module was used to analyze the influence of 9 factors (aerosol, cloud and meteorological conditions) on ACI over the YRD and the ECS, for the conditions summarized at the end of Section 4.3. These factors are summarized in Table 3, together with their q-values (Equation 2) over the ECS and the YRD. The data in Table 3 show that over the ECS, only the influences of the proxy variables CER and CF are statistically significant with $p < 0.1$. Over the YRD, the variables CER, LWP, CF, RH and LTS all exert significant impacts on ACI at the $p < 0.1$ level. However, the q-values show that the influence of these variables on the ACI values is rather weak and can explain only 10%-22% of the variation of the ACI. Furthermore, in neither of the two regions the influence of the proxy variables AOD, COT, CTP and PVV is statistically significant at the 0.1 level.

Table 3. q values for factors which may influence ACI over the ECS and the YRD, evaluated for data collected in the period from 2008-2022.

	Aerosol parameter	Cloud parameters					Meteorology parameters		
	AOD	CER	COT	LWP	CF	CTP	RH	LTS	PVV
ECS	0.06	0.14*	0.16	0.10	0.16*	0.10	0.04	0.04	0.09
YRD	0.06	0.10*	0.05	0.22*	0.21*	0.05	0.13*	0.16*	0.04

Note: * indicates that the q value is significant at the 0.1 level ($p < 0.1$).

The GDM factor detector module was also used to analyze the influence of the AOD and meteorological parameters factors (RH, LTS and PVV) on cloud properties. The results in Table 4 show that over the ECS, AOD, LTS and PVV influence all cloud parameters except CTP, with q-values which are statistically significant at the 1% level. The high q-values for AOD show that the AOD can explain 71%

(for CF) to 87% (for CER) of the variation in the cloud parameters considered in this study, which is substantially more than the explanatory power of the meteorological parameters. Among the meteorological parameters, LTS has the largest influence on cloud parameters and the effect of RH is the smallest.

Table 4. q values for factors which may influence cloud parameters over the ECS, evaluated for data collected in the period from 2008-2022.

	AOD	RH	LTS	PVV
CER	0.87***	0.36***	0.75***	0.69***
COT	0.83***	0.48*	0.79***	0.69***
LWP	0.74***	0.23	0.58***	0.56***
CF	0.71***	0.24	0.56***	0.54***
CTP	0.78	0.54	0.70	0.74

Note: ***indicates that the q value is significant at the 0.01 level ($p < 0.01$). ** indicates that the q value is significant at the 0.05 level ($p < 0.05$). * indicates that the q value is significant at the 0.1 level ($p < 0.1$).

The results from a similar analysis of the data over the YRD (Table 5) show that AOD has a statistically significant influence at the 1% level on COT and CF, but with much smaller explanatory power than over the ECS. AOD can explain 54% of the variation of CER but the statistical significance is small ($p<0.1$). Among the meteorological parameters, RH has a statistically significant influence on CTP and can explain 65% of the CTP and LTS can explain 48% of the variation of the CF with $p<0.01$. The explanatory power for the effects of RH (37%), LTS (46%) and PVV (46%) on LWP are substantial but with low statistical significance ($p<0.1$).

Table 5. q values for factors which may influence cloud parameters over the YRD, evaluated for data collected in the period from 2008-2022.

	AOD	RH	LTS	PVV
CER	0.54*	0.05	0.41	0.14
COT	0.61***	0.27	0.04	0.19
LWP	0.18	0.37*	0.46*	0.46*
CF	0.33***	0.04	0.48***	0.12
CTP	0.48	0.65***	0.22	0.38

Note: ***indicates that the q value is significant at the 0.01 level ($p < 0.01$). ** indicates that the q value is significant at the 0.05 level ($p < 0.05$). * indicates that the q value is significant at the 0.1 level ($p < 0.1$).

4.4.2 Interaction detector analysis

The interactive q-statistic values for the influence of AOD and meteorological parameters on the cloud parameters over the YRD and the ECS derived using the GDM are graphically presented in the matrix shown in Figure 7, with the q-values color coded. The data in Figure 7 show that the interactive q-values

are larger than the q-values for any of the individual parameters (Table 4). Over the ECS, the combined influences all exhibit binary nonlinear enhancement over the time period of this analysis. Calculations show that the combined effects of AOD and RH on the CER results in the highest explanatory power of 92%, as indicated by the q value (color bar at the bottom). Further inspection of the data in Figure 7

450   shows that the explanatory powers of the combined effects are high for several combinations of parameters, such as for CER combining AOD with LTS or PVV, and LTS with PVV, for COT the combination of AOD with RH, LTS or PVV or LTS with PVV, etc. The data in Figure 7 show that the combination of AOD and RH results in high explanatory power for their influence on all 5 cloud parameters and the combination of LTS with PVV has high explanatory power for their effects on CER,

455   COT and CTP.

Over the YRD, half of the interactions exhibit nonlinear enhancement of the influence of the independent parameters on the cloud properties over the time period of this analysis. The results in Figure 7 show that the combined effects of AOD and LTS on the CF result in the highest explanatory power of 0.70. The data in Fig. 7 also show that the explanatory power is largest for the combined influence of AOD together

460   with other factors, and is somewhat larger than the influence of AOD alone. What's more, the data do show that meteorological factors enhance the explanatory power of the cloud factors on cloud parameters; for example, the individual q values for the influence of AOD and PVV over the ECS were 0.83 and 0.69 but for the combined influence the q-statistic is as high as 0.90.
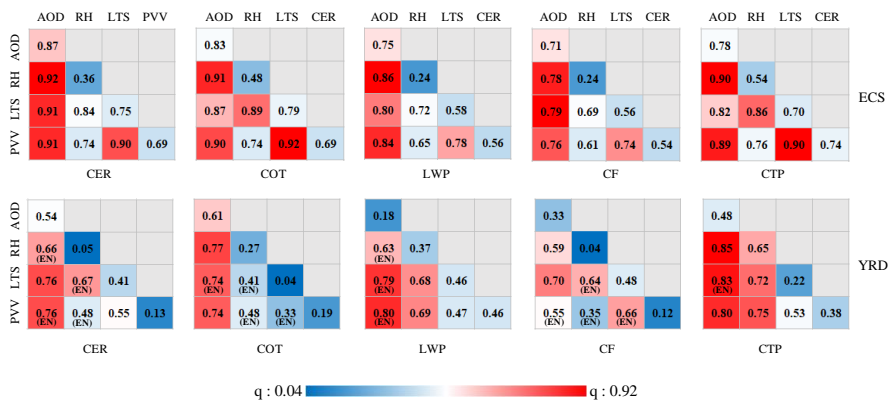
465   **Figure 7. Interactive proxy variable q-statistics over the ECS (top) and the YRD (bottom). Note: (EN) below a q value indicates the nonlinear enhancement of two variables, and no label below a q value denotes the binary enhancing of two variables (Wang and Hu, 2012).**

4.5 Behaviour of CER and other cloud properties with the increase of AOD

Scatterplots of the CER versus other cloud properties (COT, CF and CTP), with AOD as third parameter

470   (color-coded), are presented in Figure 8, over the ECS and the YRD. Over the ECS, the CER and CTP

decrease (the cloud top height increases) with the increase of AOD and the COT and CF increase. The

increase of AOD indicates an increase of the aerosol concentration and thus potentially the number of

CCN, which in turn, upon activation, results in the increase of the number of cloud droplets and thus an

increase of the COT. The positive correlation between COT and AOD over the ECS suggests that the

475   thicker clouds contain more water droplets and are formed in a more polluted atmosphere, which, as

discussed in Section 4.2, results from the influence of long-range transport of aerosol produced over land

on the aerosol burden. But at the same time, as fig. 8a shows, CER decreases with increasing AOD,

resulting in the increase in cloud albedo and thus also in the increase of COT. The increase of cloud top

height with AOD indicates that both the horizontal and vertical expansion of the clouds are also enhanced.

480   These observations are in agreement with the strong correlation between aerosol loading and cloud

vertical development for convective clouds over the North Atlantic reported by Koren et al. (2005).

In contrast to the situation over the ECS, over the YRD the increase of AOD results in an increase of the

CER and CTP (the cloud top height decreases), and a decrease of the COT. These observations are

consistent with those proposed by Liu et al. (2017) in the same study region. The decrease of the CF with

485   increasing AOD could be explained as follows. Due to the high concentration of smoke particles over the

YRD (Shen et al., 2021), aerosol particles absorb solar radiation which results in local heating of the

aerosol layer and cooling of the surface (Li et al., 2017). This in turn stabilizes the temperature profile

and reduces the relative humidity and surface moisture fluxes (evapotranspiration) (Koren et al., 2008)

and thus also cloudiness. Reduced cloud cover exposes greater areas of the aerosol layer to direct

490   irradiation from the Sun and therefore produces more intense heating of the aerosol layer, further

reducing cloudiness (Koren et al., 2008). It is noted that this process is different from that proposed by

Liu et al. (2017), i.e. that the CF increases with increasing AOD in polluted and heavily polluted

conditions (AOD>0.3). In the study of Liu et al. (2017), the LWP range was not constrained, i.e. the

aerosol-cloud interaction relationship was studied considering the whole LWP range. The data presented

495   in Table 2, shows that the ACI significantly changes between different LWP regimes, i.e. for the three

LWP intervals between 0 and 120 g m^{-2}, the ACI is negative (anti-Twomey effect) and for larger LWP it

is positive but statistically not significant. Figure 9 shows that CER and CTP substantially increase, whereas COT and CF decrease with increasing AOD in the two LWP intervals between 40-120 g m^{-2}. However, in the other three LWP intervals the relationships between these cloud parameters and AOD

500   are not evident. The different explanations offered here and in Liu et el. (2017) may be related to the different aerosol and cloud properties data sets used by Liu et al., (2017 and in the current study. On the one hand, the data sets have a different spatial resolution and cover a different time period. The dataset used in the study of Liu et al. (2017) are MYD04 Level 2 Collection 5 and MYD06 Level 2 Collection 5 in the period from 2007 to 2010. During that period the AOD over the YRD was at a maximum and

505   decreased substantially in later years (Liu et al, 2021; de Leeuw et al., 2022; 2023). On the other hand, in the study of Liu et al. (2017), the MODIS-retrieved AOD was averaged over an area with a radius of 50 km from the CALIOP target and the MODIS-retrieved cloud data were averaged within a radius of 5 km from the CALIOP target. Hence the AOD and cloud parameters were not representative for the same area, in particular in cases with inhomogeneous spatial distributions.
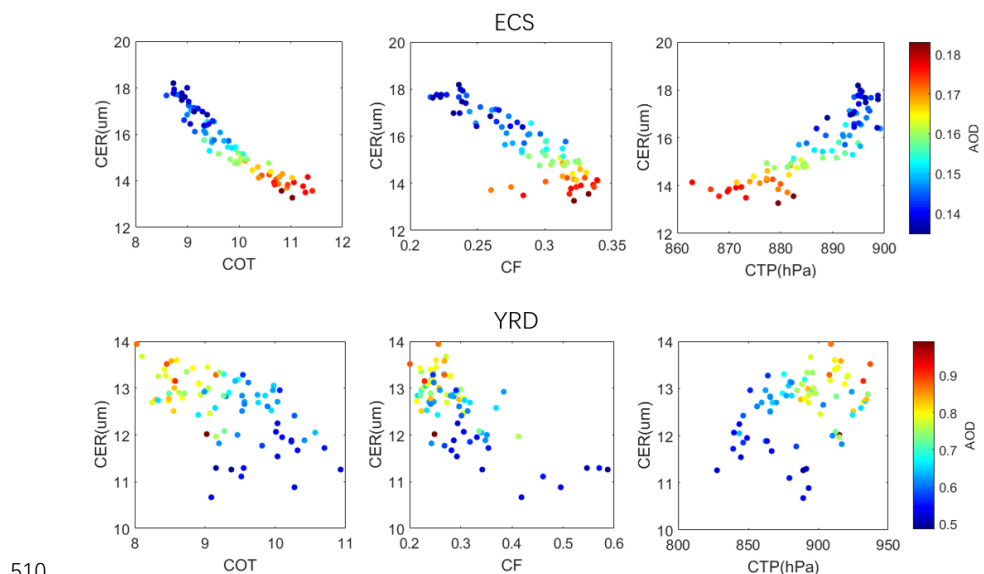
510   **Figure 8. Scatterplots of CER versus other cloud parameters (COT, CF and CTP; left to right) over the ECS (top row) and the YRD (bottom row), with AOD as third parameter, color coded following the scale at the right.**
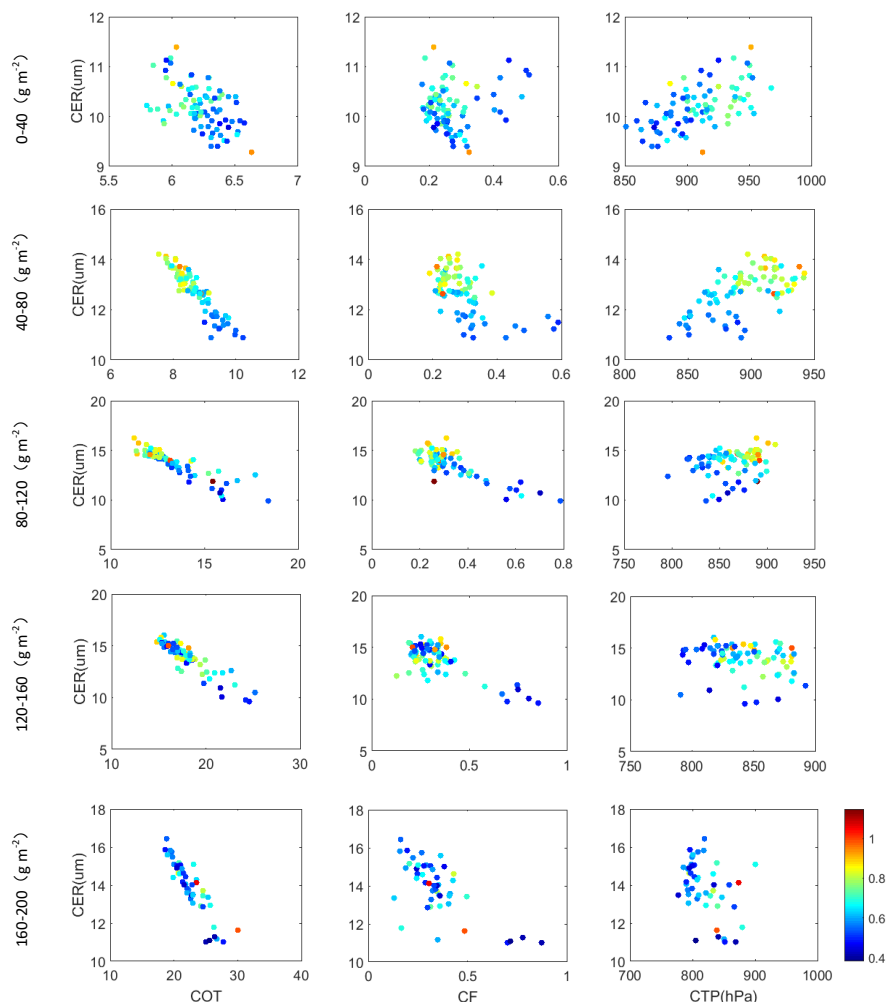
Figure 9. Scatterplots of CER versus other cloud parameters (COT, CF and CTP; left to right) over the YRD, for three different LWP intervals between 0 and 200 gm^{-2}. The AOD for each grid point is color coded following the scale at the right.

4.6 Behaviour of CER and AOD in different meteorological conditions

Scatterplots of the CER versus AOD over the ECS and the YRD, with meteorological factors (LTS, RH, PVV) (color coded) as third parameter, are presented in Figure 10. Over the ECS (Figure 10a), the AOD is inversely related to LTS, whereas the CER increases with increasing LTS. This observation is different from the findings of Saponaro et al. (2017) who reported that there is no significant influence of

atmospheric stability (LTS) on the relationship between CER and AOD. Likewise, the AOD is inversely

related to RH whereas CER increases with increasing RH. These two observations indicate that RH and

525 LTS have a similar effect on the relationship between AOD and CER. In contrast, with the increase of

PVV, the AOD becomes larger but the CER becomes smaller. The CER vs AOD curves show that, overall,

the meteorological conditions do not change the functional relationship between AOD and CER, but

quantitatively they do have an effect. The change of meteorological conditions plays an important role

in the variation of CER. In addition, Figure 10b shows that, over the ECS, with the increase of the aerosol

530 concentrations, the number of cloud condensation nuclei also increases, so the same amount of water

vapor is distributed over a larger number of cloud droplets resulting in smaller cloud droplets. Hence, the

interaction between AOD and CER over the ECS is in agreement with the Twomey effect.

Cloud properties as a function of AOD for two different LTS conditions over the YRD are presented in

figure 10d, i.e. for low LTS, with a mean value of 13.27 representing an unstable atmosphere; and for

535 high LTS, with a mean value of 15.23 representing a stable atmosphere. In unstable atmospheric

conditions the CER is larger than in stable conditions, and in both unstable and stable conditions CER

increases with AOD. The larger CER in unstable conditions may be due to better vertical mixing of both

aerosol particles and water vapor (Liu et al., 2017).

The effect of relative humidity (RH, at 750 hPa) on the relationship between the cloud properties and

540 AOD is evaluated by dividing the data into two equally sized subsets for high and low RH, and the mean

relative humidity values for each subset are calculated. In high relative humidity conditions (57%) the

CER is much larger than in low relative humidity conditions (48%), as shown in Fig. 10e.

The effect of vertical velocity (PVV) on the CER in polluted and heavily polluted conditions is weak. In

general, the influence of aerosol concentration (AOD) on the CER is larger than that of meteorological

545 conditions, although the combined effect of AOD and meteorological conditions is larger than that of

AOD alone (Fig. 7). Therefore, aerosol concentration plays a dominant role in the effects of different

factors on CER.
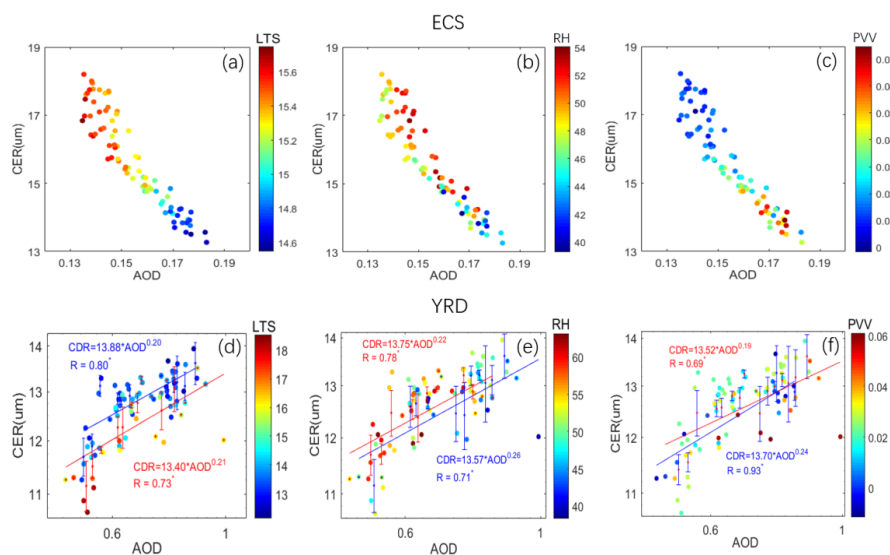
Figure 10. Scatterplots of CER versus meteorological parameters (LTS, RH and PVV; left to right) over the
550 **ECS (top row) and the YRD (bottom row). The AOD for each grid point is color coded following the scale at the right. The lines in the bottom row (YRD) present the least-square fits for low and high LTS, RH and PVV, respectively, as described in the text, and the resulting relations are presented in each figure. The marker ∗ at the top right corner of R value denotes statistically significant if p < 0.05.**

5 Conclusions

555   Warm cloud properties over eastern China have been investigated in relation to aerosol and meteorological conditions using 15 years (2008-2022) of data from passive (MODIS/Aqua) satellite measurements, together with ERA Interim Reanalysis meteorological data. The Yangtze River Delta, a heavily polluted region in eastern China, and the East China Sea with a relatively clean atmosphere, were selected as study areas. Relationships between cloud droplet effective radius and AOD (used as a proxy

560   for aerosol concentration), characterized by the aerosol cloud interaction (ACI) index, were constructed for different constraints of AOD and LWP. The effects of AOD on CER were investigated for three AOD regimes. In view of the uncertainty of MODIS-retrieved AOD and the scatter in the CER/AOD relations, data for AOD<0.1 were not considered in this study. In the AOD regime 0.1 to 0.3, the CER over the YRD did not change significantly with AOD, whereas over the ECS the CER strongly decreased with

565   AOD and the derived relationship between CER and AOD is statistically significant. In the third AOD regime, with AOD > 0.3, over the YRD the CER increased with increasing AOD, whereas over the ECS the CER did not significantly change as function of AOD, although the variations in the CER increased

with AOD, especially for higher AOD (> ~0.8). Based on these results, two different AOD regimes were selected for further investigation of the ACI: 0.1<AOD<0.3 over the ECS and AOD > 0.3 over the YRD.

570   The spatial distribution of ACI, here defined as the change in CER as a function of AOD (eq. 1), averaged over the 15-years study period, shows that it was negative and statistically significant over the ECS and positive over the YRD. These results were obtained using data with no restriction on LWP. Further selection of the data in different LWP intervals shows that over the YRD, for AOD greater than 0.3, ACI is negative for LWP in the interval [0-120 g m^{-2}] with very small differences between three LWP intervals

575   (0-40, 40-80 and 80-120 g m^{-2}). In contrast, over the ECS, for AOD in the range from 0.1 to 0.3, ACI is positive in the LWP interval [40-200 g m^{-2}] and there are substantial differences between the 4 LWP intervals, with ACI increasing with LWP, as shown in Table 2.

By using the geographical detector method, the influence of different parameters (AOD and meteorological parameters) on the cloud properties in eastern China has been investigated. Over the ECS,

580   AOD has the largest influence on cloud parameters, as indicated by the large and significant q values. Among the meteorological factors, LTS has more influence on the variations of the cloud parameters than RH and PVV. Over the YRD, AOD has the largest influence on CER and COT, with large and significant q values. Among the meteorological factors, the effect of LTS on CF is greater than that of RH and PVV. The interactive q-statistic values derived in this study were larger than any of the values

585   for single variables. The combined influences of AOD and meteorological parameters exhibit binary nonlinear enhancement of the explanatory power of the variation of the cloud parameters.

The response of different cloud parameters to variations in AOD and in meteorological conditions has been analyzed. Over the ECS, with the increase of the AOD, the CER and CTP decrease, and the COT and CF increase. Over the YRD, with the increase of the AOD, the CER and CTP increase, and the COT

590   and cloud cover decrease. The CER is larger in unstable atmospheric conditions than in stable conditions, irrespective of the AOD. The cloud fraction is much larger in high relative humidity conditions than in low relative humidity conditions. However, the impact of vertical velocity on the CER is weak in polluted and heavily polluted conditions. In general, the influence of the AOD on the CER is greater than that of meteorological conditions. Therefore, AOD plays a dominant role in the effects of different factors on

595   CER.

Different from previous studies, here the interaction between aerosol and CER has been investigated by

considering different AOD and LWP regimes on ACI over land and ocean. The relative importance of AOD and meteorological parameters on cloud properties were examined by using the geographical detector method. The results of this study contribute to improve the understanding of the indirect effects of aerosols and the role of various driving factors on the cloud microphysical properties. They provide a reference for improving the parameterization scheme of regional climate models in eastern China.

Data availability

All data used in this study are publicly available. The satellite data from the MODIS instrument used in this study were obtained from https://ladsweb.nascom.nasa.gov/search/ (last access: 12 July 2022, Liu, 2022a). The the ECMWF ERA-5 reanalysis data were collected from the ECMWF ERA-5 reanalysis data server https://cds.climate.copernicus.eu/cdsapp#!/dataset/reanalysis-era5-pressure-levels-monthly-means?tab=form (last access: 12 July 2022, Liu, 2022b).

Author contributions

YL and GL designed the research. YL led the analyses. YL and LT wrote the manuscript with major input from JH, GL and further input from all other authors. All authors contributed to interpreting the results and to the finalization and revision of the manuscript.

Competing interests

The authors declare that they have no conflict of interest.

Acknowledgements

This work was supported by the National Natural Science Foundation of China (Grant No. 42001290), and the Natural Science Foundation of China (Grant No. 41871253). We are grateful for the easy access to MODIS data products provided by NASA. We also thank ECMWF for providing daily ERA-Interim reanalysis data. The study contributes to the ESA / MOST cooperation project DRAGON5, Topic 3 Atmosphere, sub-topic 3.2 Air-Quality.

620 **References**

Andreae, M. O.: Correlation between cloud condensation nuclei concentration and aerosol optical thickness in remote and polluted regions, Atmos. Chem. Phys., 9, 543-556, https://doi.org/10.5194/acp-9-543-2009, 2009.

Albrecht, B. A.: Aerosols, cloud microphysics, and fractional cloudiness, Science, 245, 1227-1230, 1989.

625 Bellouin, N., Quaas, J., Gryspeerdt, E., Kinne, S., Stier, P., Watson-Parris, D., et al.: Bounding global aerosol radiative forcing of climate change. Reviews of Geophysics, 58, e2019RG000660. https://doi.org/10. 1029/2019RG000660, 2020.

Brewer CA, Pickle L.: Evaluation of methods for classifying epidemiological data on choropleth maps in series. Annals of the Association of American Geographers, 92(4), 662–81, 2002.

630 Burrows, J. P., Platt, U., Borrell, P.: The remote sensing of tropospheric composition from space, Springer Verlag, Heidelberg, Germany, 2011.

Christensen, M. W., Jones, W. K., Stier, P.: Aerosols enhance cloud lifetime and brightness along the stratus-to-cumulus transition, Proceedings of the National Academy of Sciences, 117(30), 17591-17598.

Chen, Y.-C., Christensen, M. W., Stephens, G. L., and Seinfeld, J. H.: Satellite-based estimate of global

635 aerosol-cloud radiative forcing by marine warm clouds, Nat. Geosci., 7, 643–646, https://doi.org/10.1038/ngeo2214, 2014.

Christensen, M. W., Chen, Y.-C., and Stephens, G. L.: Aerosol indirect effect dictated by liquid clouds, J. Geophys. Res., 121, 14636–14650, https://doi.org/10.1002/2016JD025245, 2016.

Costantino, L. and Bréon, F. M.: Analysis of aerosol-cloud interaction from multi-sensor satellite

640 observations. Geophys. Res. Lett., 37, L11801, doi:10.1029/2009GL041828, 2010.

Costantino, L. and Bréon, F. M.: Aerosol indirect effect on warm clouds over South-East Atlantic, from co-located MODIS and CALIPSO observations, Atmos. Chem. Phys., 13: 69-88, 2013.

de Leeuw, G., Andreas, E. L., Anguelova, M. D., Fairall, C. W., Lewis, E. R., O'Dowd, C., Schulz,M, and Schwartz, S. E. Schwartz.: Production flux of sea spray aerosol, Rev. Geophys., 49, RG2001,

645 doi:10.1029/2010RG000349, 2011.

de Leeuw, G., Sogacheva, L., Rodriguez, E., Kourtidis, K., Georgoulias, A. K., Alexandri, G., Amiridis, V., Proestakis, E., Marinou, E., Xue, Y., and van der A, R.: Two decades of satellite observations of

AOD over mainland China using ATSR-2, AATSR and MODIS/Terra: data set evaluation and large-scale patterns, Atmos. Chem. Phys., 18, 1573-1592, https://doi.org/10.5194/acp-18-1573-2018, 2018.

650   Fan J, Wang Y, Rosenfeld D, et al.: Review of aerosol-cloud interactions: Mechanisms, significance, and challenges. Journal of the Atmospheric Sciences,73(11): 4221-4252, 2016.

de Leeuw, G., Fan, C, Li, Z., Dong, J., Li, Y., Ou, Y., and Zhu, S. (2022). Spatiotemporal variation and provincial scale differences of the AOD across China during 2000–2021. Atmospheric Pollution Research 13 (2022) 101359 (14 pp). https://doi.org/10.1016/j.apr.2022.101359.

655   de Leeuw, G., Kang, H., Fan, C., Li, Z., Fang, C., Zhang, Y. (2023). Meteorological and anthropogenic contributions to changes in the Aerosol Optical Depth (AOD) over China during the last decade. Atm. Env., 301, 119676. https://doi.org/10.1016/j.atmosenv.2023.119676.

Feingold, G., Remer, L. A., Ramaprasad, J., Kaufman, Y. J.: Analysis of smoke impact on clouds in Brazilian biomass burning regions: an extension of Twomey's approach, J. Geophys. Res., 106 (D19),

660   22907-22922, 2001.

Grandey, B.S., Stier, P.: A critical look at spatial scale choices in satellite-based aerosol indirect effect studies. Atmos. Chem. Phys., 10, 11459-11470, 2010.

Gryspeerdt, E., Stier, P., and Partridge, D. G.: Satellite observations of cloud regime development: the role of aerosol processes, Atmos. Chem. Phys., 14, 1141-1158, doi:10.5194/acp-14-1141-2014, 2014.

665   Huang, H., Thomas, G. E., and Grainger, R. G.: Relationship between wind speed and aerosol optical depth over remote ocean, Atmos. Chem. Phys., 10, 5943-5950, https://doi.org/10.5194/acp-10-5943-2010, 2010.

Jia, H. L., Ma, X. Y., Quaas, J., Yin, Y., Qiu, T.: Is positive correlation between cloud droplet effective radius and aerosol optical depth over land due to retrieval artifacts or real physical processes?

670   Atmospheric Chemistry and Physics, 19, 13, 8879-8896, 2019.

Jin, M. L. and Shepherd, J. M.: Aerosol relationships to warm season clouds and rainfall at monthly scales over east China: Urban land versus ocean, J. Geophys. Res., 113, D24S90, https://doi.org/10.1029/2008JD010276, 2008.

Kaufman, Y.J. and Fraser, R.S.: The effect of smoke particles on clouds and climate forcing. Science,

675   1997. 277(5332): p. 1636-1639.

Klein, S. A. and Hartmann, D. L.: The seasonal cycle of low stratiform clouds, J. Climate, 6, 1587-1606, 1993.

Koren, I., Kaufman, Y. J., Rosenfeld, D., Remer, L. A., Rudich, Y.: Aerosol invigoration and restructuring of Atlantic convective clouds. Geophys. Res. Lett., 32 (14), L14828, 2005.

680 Koren, I., Martins, J. V., Remer, L. A., and Afargan, H.: Smoke invigoration versus inhabitation of clouds over the Amazon, Science, 321, 946-949, doi:10.1126/science.1159185, 2008.

Kourtidis, K., Stathopoulos, S., Georgoulias, A. K., Alexandri, G., and Rapsomanikis, S.: A study of the impact of synoptic weather conditions and water vapor on aerosol-cloud relationships over major urban clusters of China, Atmos. Chem. Phys., 15, 10955-10964, doi:10.5194/acp-15-10955-2015, 2015.

685 Levy, R. C., Mattoo, S., Munchak, L. A., Remer, L. A., Sayer, A. M., Patadia, F., and Hsu, N. C.: The Collection 6 MODIS aerosol products over land and ocean, Atmos. Meas. Tech., 6, 2989-3034, https://doi.org/10.5194/amt-6-2989-2013, 2013.

Li, Z. Q., Guo, J. P., Ding, A. J., Liao, H., Liu, J. J., Sun, Y. L., Wang, T. J., Xue, H. W., Zhang, H. S., Zhu, B.: Aerosol and boundary-layer interactions and impact on air quality. National Science Review 4:

690 810-833, 2017, doi: 10.1093/nsr/nwx117, 2017.

Liu, Y. Q.: MODIS L3 collection 6.1 data, Institute of Urban Environment, Chinese Academy of Sciences, available at: https: //ladsweb.nascom.nasa.gov/search/, last access: 12 July 2022a.

Liu, Y. Q.: ECMWF ERA-5 reanalysis data set, Institute of Urban Environment, Chinese Academy of Sciences, available at: https://cds.climate.copernicus.eu/cdsapp#!/dataset/reanalysis-era5-pressure-

695 levels-monthly-means?tab=form, last access: 12 July 2022b.

Liu, Y., de Leeuw, G., Kerminen, V.-M., Zhang, J., Zhou, P., Nie, W., Qi, X., Hong, J., Wang, Y., Ding, A., Guo, H., Krüger, O., Kulmala, M., and Petäjä, T.: Analysis of aerosol effects on warm clouds over the Yangtze River Delta from multi-sensor satellite observations, Atmos. Chem. Phys., 17, 5623–5641, https://doi.org/10.5194/acp-17-5623-2017, 2017.

700 Liu, Q., Duan, S. Y., He, Q. S., Chen, Y. H., Zhang, H., Cheng, N. X., Huang, Y. W., Chen, B., Zhan, Q. Y., Li, J. Z.: The variability of warm cloud droplet radius induced by aerosols and water vapor in Shanghai from MODIS observations, Atmospheric Research, 253, 105470, 2021.

Liu, T. Q., Liu, Q., Chen, Y. H., Wang, W. C., Zhang, H., Li, D., Sheng, J.: Effect of aerosols on the macro- and micro-physical properties of warm clouds in the Beijing-Tianjin-Heibei region. Science of the Total Environmen, 720, 137618, 2020.

Liu, Y., Zhang, J., Zhou, P., Lin, T., Hong, J., Shi, L., Yao, F., Wu, J., Guo, H., and de Leeuw, G.: Satellite-based estimate of the variability of warm cloud properties associated with aerosol and meteorological conditions, Atmos. Chem. Phys., 18, 18187-18202, https://doi.org/10.5194/acp-18-18187-2018, 2018.

Liu, Y., de Leeuw, G., Kerminen, V.-M., Zhang, J., Zhou, P., Nie, W., Qi, X., Hong, J., Wang, Y., Ding, A., Guo, H., Krüger, O., Kulmala, M., and Petäjä, T.: Analysis of aerosol effects on warm clouds over the Yangtze River Delta from multi-sensor satellite observations, Atmos. Chem. Phys., 17, 5623-5641, https://doi.org/10.5194/acp-17-5623-2017, 2017.

Liu, Y., Lin, T., Hong, J., Wang, Y., Shi, L., Huang, Y., Wu, X., Zhou, H., Zhang, J., and de Leeuw, G. (2021). Multi-dimensional satellite observations of aerosol properties and aerosol types over three major urban clusters in eastern China, Atmos. Chem. Phys., 21, 12331–12358, https://doi.org/10.5194/acp-21-12331-2021, 2021.

Lohmann, U., Rotstayn, L., Storelvmo, T., Jones, A., Menon, S., Quaas, J., Ekman, A.M.L., Koch, D., Ruedy, R.: Total aerosol effect: radiative forcing or radiative flux perturbation? Atmospheric Chemistry and Physics, 10 (7): p. 3235-3246, 2010.

Matheson, M. A., Coakley Jr., J. A., and Tahnk, W. R.: Aerosol and cloud property from relationships for summer stratiform clouds in the northeastern Atlantic from advanced very high resolution radiometer observations, J. Geophys. Res., 110, D24204, doi:10.1029/2005JD006165, 2005.

Meskhidze, N., Nenes, A.: Effects of ocean ecosystem on marine aerosol-cloud interaction. Adv. Meteorol, doi:10.1155/2010/239808, 2010.

Michibata, T., Kawamoto, K., and Takemura, T.: The effects of aerosols on water cloud microphysics and macrophysics based on satellite-retrieved data over East Asia and the North Pacific, Atmos. Chem. Phys., 14, 11935-11948, https://doi.org/10.5194/acp-14-11935-2014, 2014.

Pandey, S. K., Vinoj, V., Panwar, A.: The short-term variability of aerosols and their impact on cloud properties and radiative effect over the Indo-Gangetic Plain. Atmospheric Pollution Research, 11, 630-638, 2020.

Qiu, Y, Zhao, C., Guo, J., Li, J.: 8-Year ground-based observational analysis about the seasonal variation of the aerosol-cloud droplet effective radius relationship at SGP site. Atmospheric Environment 164 139-146, 2017. http://dx.doi.org/10.1016/j.atmosenv.2017.06.002.

735 Quaas, J., Boucher, O., Bellouin, N., Kinne, S.: Satellite-based estimate of the direct and indirect aerosol climate forcing, J. Geophys. Res., 113, D05204, doi:10.1029/2007JD008962, 2008.

Rao, S., Dey, S.: Consistent signal of aerosol indirect and semi-direct effect on water clouds in the oceanic regions adjacent to the Indian subcontinent. Atmospheric Research, 232, 2020.

Remer, L. A., Kaufman, Y. J., Tanre, D., Mattoo, S., Chu, D. A., Martins, J. V., Li, R. R., Ichoku, C.,

740 Levy, R. C., Kleidman, R. G., Eck, T. F., Vermote, E., and Holben, B. N.: The MODIS aerosol algorithm, products, and validation, J. Atmos. Sci., 62, 947–973, https://doi.org/10.1175/JAS3385.1, 2005.

Rosenfeld, D. and Lensky, I. M.: Satellite-based insights into precipitation formation processes in continental and maritime convective clouds, B. Am. Meteorol. Soc., 79, 2457-2476, 1998.

Rosenfeld, D., Andreae, M. O., Asmi, A., Chin, M., de Leeuw, G., Donovan, D., Kahn, R., Kinne, S.,

745 Kivekäs, N., Kulmala, M., Lau, W., Schmidt, S., Suni, T., Wagner, T., Wild, M., and Quaas, J.: Global observations of aerosol-cloudprecipitation- climate interactions, Rev. Geophys., 52, 750-808, doi:10.1002/2013RG000441, 2014.

Rosenfeld, D., Zhu, Y. N., Wang, M. H., Zheng, Y. T., Goren, T., Yu, S. C.: Aerosol-driven droplet concentrations dominate coverage and water of oceanic low-level clouds, Science, 363, 6427, 2019.

750 Saponaro, G., Kolmonen, P., Sogacheva, L., Rodriguez, E., Virtanen, T., de Leeus, G.: Estimates of the aerosol indirect effect over the Baltic Sea region derived from 12 years of MODIS observations, Atmos. Chem. Phys., 17, 3133-3143, 2017.

Sayer, A. M., Munchak, L. A., Hsu, N. C., Levy, R. C., Bettenhausen, C., and Jeong, M. J.: MODIS Collection 6 aerosol products: Comparison between Aqua's e-Deep Blue, Dark Target, and "merged"

755 data sets, and usage recommendations, J. Geophys. Res.-Atmos., 119, 13965-13989, https://doi.org/10.1002/2014jd022453, 2014.

Seinfeld, J.H.; Pandis, S.N. Atmospheric Chemistry and Physics: From Air Pollution to Climate Change; John Wiley and Sons, Inc.: New York, 1998; ISBN 0-471-17815-2.

Shen, L. J., Wang, H. L., Kong, X. C., Zhang, C., Shi, S. S., Zhu, B.: Characterization of black carbon

760   aerosol in the Yangtze River Delta, China Seasonal variation and source apportionment, Atmospheric

Pollution Research, 12, 195-209, 2021.

Shao, H. F and Liu, G. S.: Why is the satellite observed aerosol's indirect effect so variable?, Geophysical

research letters, 32, L15802, doi:10.1029/2005GL023260, 2005.

Slingo, A.: Sensitivity of the Earth's radiation budget to changes in low clouds, Nature, 343(6253), 49-

765   51, 1990.

Smirnov, A., Sayer, A. M., Holben, B. N., Hsu, N. C., Sakerin, S. M., Macke, A., Nelson, N. B.,

Courcoux, Y., Smyth, T. J., Croot, P., Quinn, P. K., Sciare, J., Gulev, S. K., Piketh, S., Losno, R., Kinne,

S., and Radionov, V. F.: Effect of wind speed on aerosol optical depth over remote oceans, based on data

from the Maritime Aerosol Network, Atmos. Meas. Tech., 5, 377–388, https://doi.org/10.5194/amt-5-

770   377-2012, 2012.

Sogacheva, L., Popp, T., Sayer, A. M., Dubovik, O., Garay, M. J., Heckel, A., Hsu, N. C., Jethva, H.,

Kahn, R. A., Kolmonen, P., Kosmale, M., de Leeuw, G., Levy, R. C., Litvinov, P., Lyapustin, A., North,

P., Torres, O., and Arola, A.: Merging regional and global aerosol optical depth records from major

available satellite products, Atmos. Chem. Phys., 20, 2031-2056, https://doi.org/10.5194/acp-20-2031-

775   2020, 2020.

Su, W., Loeb, N. G., Xu, K.-M., Schuster, G. L., and Eitzen, Z. A.: An estimate of aerosol indirect effect

from satellite measurements with concurrent meteorological analysis, J. Geophys. Res.-Atmos., 115,

D18219, doi:10.1029/2010JD013948, 2010.

Tao, W. K., Chen, J. P., Li, Z., Wang, C. E., Zhang, C. D.: Impact of aerosols on convective clouds and

780   precipitation, Reviews of Geophysics, 50(2), 2012.

Ten Hoeve, J. E., Remer, L. A., and Jacobson, M. Z.: Microphysical and radiative effects of aerosols on

warm clouds during the Amazon biomass burning season as observed by MODIS: impacts of water vapor

and land cover, Atmos. Chem. Phys., 11, 3021-3036, doi:10.5194/acp-11-3021-2011, 2011.

Twomey, S.: The influence of pollution on the shortwave albedo of clouds, J. Atmos. Sci. 34(7), 1149-

785   1152, 1977.

Wang, J. F., Li, X. H., Christakos, G., Liao, Y. L., Zhang, T., Gu, X., Zheng, X. Y.: Geographical detectors-based health risk assessment and its application in the neural tube defects study of the Heshun Region, China. Int. J. Geogr. Inf. Sci. 24, 107-127, 2010.

Wang, J. F., Hu, Y.: Environmental health risk detection with GeogDetector. Environ. Model. Softw. 33, 790   114-115, 2012.

Wang, J. F., Zhang, T. L., Fu, B. J.: A measure of spatial stratified heterogeneity. Ecol. Indic. 67, 250-256, 2016.

Wang, J. X., Hu, M. G., Zhang, F. S., Gao, B. B.: Influential factors detection for surface water quality with geographical detectors in China. Stoch. Environ. Res. Risk A 32, 2633-2645, 2018.

795   Wang, F., Guo, J., Zhang, J., Huang, J., Min, M., Chen, T., Liu, H., Deng, M., Li, X.: Multi-sensor quantification of aerosol-induced variability in warm clouds over eastern China, Atmos. Environ., 113: 1-9, 2015. http://dx.doi.org/10.1016/j.atmosenv.2015.04.063.

Wood, R. and Bretherton, C. S.: On the relationship between Stratiform Low Cloud Cover and Lower-Tropospheric Stability, J. Climate, 19, 6425-6432, 2006.

800   Zhao, C. F., Qiu, Y. M., Dong, X. B., Wang, Z. E., Peng, Y. R., Li, B. D., Wu, Z. H., Wang, Y.: Negative aerosol-cloud re relationship from aircraft observations over Hebei, China. Earth and Space Science, 5, 19-29, 2018.

Zhang, X. L., Zhao, Y.: Identification of the driving factors' influences on regional energy-related carbon emissions in China based on geographical detector method. Environ. Sci. Pollut. Res. 25, 9626-9635, 805   2018.

Zhou, C. S., Chen, J., Wang, S. J.: Examining the effects of socioeconomic development on fine particulate matter (PM2.5) in China's cities using spatial regression and the geographical detector technique. Sci. Total Environ. 619, 436-445, 2018.

Yuan, T., Li, Z., Zhang, R., and Fan, J.: Increase of cloud droplet size with aerosol optical depth: an 810   observation and modeling study, J. Geophys. Res., 113, D04201, doi:10.1029/2007JD008632, 2008.